Eurasian Journal of Analytical Chemistry
ISSN: 1306-3057 OPEN ACCESS 2020 15 (1): 32-44

Ag Doped Hydroxyapatite Nano Particles for Removal of Methyl Red Azo Dye from Aqueous Solutions (Kinetic and Thermodynamic Studies

Atena Dehghanpoor Frashah, Saeedeh Hashemian*, Fatemeh Tamadon

Received: 11 December 2019 ▪ Revised: 03 January 2020 ▪ Accepted: 15 January 2020

Abstract: Hydroxyapatite (HA) and Ag doped nano HA ($Ca_{9.8}Ag_{0.2}$ $(PO_4)_6(OH)_2$) was prepared by precipitation method. For characterization FTIR, SEM, EDX, BET and XRD methods were used. Adsorption of methyl red (MR) by (HA) and Ag doped nano HA was investigated. Ag doped nano HA had higher adsorption capacity for MR. The pseudo second order model provided better fit to experimental data in the kinetic studies. Based on the sum of squares errors (SSE), the Freundlich isotherm better fits sorption data than the Langmuir equation. The negative values of ΔG^{o} and positive value of ΔH^{o} indicated spontaneous and endothermic adsorption process. The Ag doped nano HA wasreusable sufficient sorbent.

Keywords: Adsorption, Ag Doped, Hydroxyapatite (HA), Methyl Red, AZO Dye.

INTRODUCTION

Textile, paper, plastics, and cosmetic industries use wide variety of dyes to color their products. The wastewaters containing dyes are very difficult to treat, since the dyes are recalcitrant molecules (particularly azo dyes), resistant to aerobic digestion and are stable to oxidizing agents. Synthetic dyes usually have complex aromatic molecular structure. Discharge large amount of effluents including dyes which are very toxic and could cause serious ecological problems. Therefore, dye pollution in water stream is a major environmental problem. Different methods for dye removal from industrial wastewaters such as such biological treatment (Kornaros, and Lyberatos,2006), coagulation, electrochemical techniques (Gadekar and Ahammed, 2016, Pan et al. 2013, Nourmoradi, et al. 2015), oxidation [5-8] and adsorption [9-13] were examined. It has been reported that many different types of adsorbents are effective in removing azo dyes from aqueous effluents [14-16].

Hydroxyapatite (HA) has the chemical formula of $Ca_{10}(PO_4)_6(OH)_2$. It is well-known inorganic material in the biological and medical fields. HA has a specific adsorption property against organic substances. It is used as an adsorbent for removal of heavy metals and dyes. HA has low water solubility, high stability under reducing and oxidizing conditions, high specific surface area and good buffering properties [17, 18]. Utilizing the adsorption properties HA is expected to be a useful material that cleans to environment.

Application of hydroxyapatiteas drug carrier was studied [19-21]. Yin et al. studied the adsorption of histatins 1,3 and 5 by HA and concluded that histatin 5 could be impaired by mineral adsorption [22].Degradation of antibiotics of ciprofloxacin by zincoxide hydroxyapatite was examined [23].The natural and synthetic apatites for the removal of metals from aqueous solutions were reported by Dybowska et al. [24]. The removal of different metal ions such as Cu^{+2},Zn^{2+}, Cd^{2+} and Pb^{2+} using hydroxyapatite has studied and results showed that HA had high sorption capacity for metal ions removal[25-28].HA also was examined for adsorptive properties of dye and organic compounds [29, 30].

Suzuki et al. have found calcium ions of HA can be exchanged with various metals ions in aqueous media [31]. The substituted impurities play important role in the biological responses of bone cells. The presence of several ionic substitutions such as F^{-}, Na^{+}, Mg^{+2}, Ag^{+} in the lattice of HA causes the change in space group, morphology, stability, and mechanical properties of the HA structure. The most antibacterial

Atena Dehghanpoor Frashah, Department of Chemistry, Yazd Branch, Islamic Azad University, Yazd, Iran.
Saeedeh Hashemian*, Department of Chemistry, Yazd Branch, Islamic Azad University, Yazd, Iran.
E-mail: Sa_hashemian@iauyazd.ac.ir
Fatemeh Tamadon, Department of Chemistry, Yazd University, Yazd, Iran.

inorganic materials are the ceramics immobilizing antibacterial metals, such as silver and copper. Silver, is known as a disinfectant for many years, has a broad spectrum of antibacterial activity and exhibits low toxicity toward mammalian cells. From the view point of biomedical engineering, the silver is well known for its broad spectrum antibacterial effect at very low concentrations, and it possesses many advantages, such as good antibacterial ability, excellent biocompatibility, and satisfactory stability. The scientific literature points to the wide use of silver in numerous applications [32, 33].

The first aim of this study is to prepare and characterize nano-HA and Ag doped HA. The second goal is investigation of potential use of nano-HA and Ag doped HA as an efficient adsorbent in the treatment of wastewater for dye removal.

EXPERIMENTAL

Materials and Methods

All chemical used were of analytical grade purity and were used as received without any purification. The all of chemicals were purchased from Merck chemical co (Germany). Distillated water was used in all of experiments.

Methyl red (2-(*N*,*N*-dimethyl-4-aminophenyl) azobenzenecarboxylic acid), CAS number 493-52-7 with chemical formula of $C_{15}H_{15}N_3O_2$ (MR) as a sample of pollutant was used. It has molecular weight of 269.30 g mol^{-1} (Fig. 1). The standard solution of MR 1000 mg L^{-1} was prepared and subsequently whenever necessary diluted.

HA and substituted HA was prepared by aqueous precipitation. HA was synthesized by double decomposition according to the procedure described by Rey [34, 35].A solution composed of 35.4 g of $Ca(NO_3)_2{\cdot}4H_2O$ in 0.5 L of distilled water was immediately poured at room temperature into a solution composed of 34.8 g of di-ammonium hydrogen phosphate $(NH_4)_2HPO_4$ in 1 L of distilled water. The pH of solution was adjusted to seven by ammonia solution. After low agitation for 2 h, the suspension was briefly filtered on a large Büchner funnel, washed with distilled water, dried at 100 °C for 48 h and sieved.

Ag doped HA nanoparticles($Ca_{9.8}Ag_{0.2}(PO_4)_6(OH)_2$), were performed by setting the atomic ratio of Ag/[Ag + Ca] at 20% and [Ca + Ag]/P as 1.67. The $AgNO_3$ and $Ca(NO_3)_2{\cdot}4H_2O$ were dissolved in deionized water to obtain 300 mL [Ca+ Ag]-containing solution. On the other hand, Ag dopedHA was prepared as the same procedure, but instead of Ca ions, % 2 Ag ions were used. After the reaction, the deposited mixtures were washed several times with deionized water. The resulting material was dried at 100°C for 48 h.

All pH measurements were carried out with an ISTEK- 720P pH meter (Germany). UV-Vis spectrophotometer 160-A Shimadzu (Japan) was used for determination of concentration of MR. IR measurements were performed by FTIR tensor-27 of Burker Co., (Germany) using the KBr pellet between the ranges 500 to 4000 cm^{-1}. The powder X–ray diffraction studies were made on a Philips PW1840 (Netherlands) diffractometer using Ni-filtered Cu k_α radiation of wave length 1.54060 A°. The average particle size and morphology of samples were observed by SEM using a Hitachi S-3500 Scanning Electron Microscope (Japan).

The specific surface area was measured by N_2 adsorption–desorption isotherm and was obtained with an ASAP- 2010 instrument (Micromeritics). The pore size distribution was determined by The BJH (Barret–Joyner–Hallender) method. Mean pore diameter and total pore volume calculated by the BET (Brunauer–Emmett–Teller) equation.

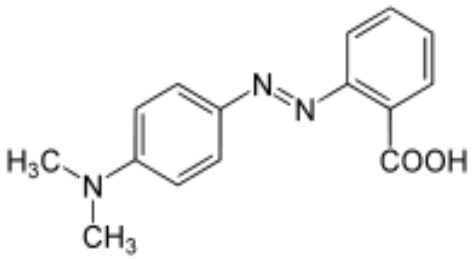

Fig. 1: Chemical structure of MR

Adsorption Experiments

For investigating of effect of different parameters like; the contact time, pH and sorbent dosage on the sorption capacity of MR, various experiments have been carried out. All experiments were conducted at

room temperature. 0.1 g of sorbent was added in 30 ml MR on rotary shaker at a constant speed of 150 rpm. After different contact times (0–120 min), the sorbent was removed from the solution and the equilibrium concentration of MR in the solution was determined with UV spectrophotometer at the wavelength 410 nm (λ_{max}).To optimize the sorbent dosage, different amounts of the sorbents were examined. A known amount of sorbent (0.01–0.2 g) was added to 30 mL of MR solutions. To study the effect of solution pH, 0.10 g of HA was agitated with 30 mL of dye solution of 50 mg L^{-1} at different pHs (2-12) using water-bath shaker at room temperature. The pH was adjusted by adding a few drops of diluted 0.1N NaOH or 0.1N HCl. Each experiment was repeated five times, and the average results were given. Relative standard deviation (% RSD) was determined between 1.93 and 2.88 % for each points at all the experiments.

The percent removal of MR by the hereby adsorbent is given by:

$$\% \text{ adsorption} = [(C_0-C_e)/C_0] \times 100 \qquad (1)$$

Where, C_0, C_e is denoted the initial and equilibrium concentration of MR dye (mg L^{-1}), respectively.

The amount of equilibrium adsorption, q_e (mg g^{-1}), was calculated by:

$$q_e = (C_0-C_e)V/W \qquad (2)$$

Where, C_0 and C_e (mg L^{-1}) are the liquid-phase concentrations of dye at initial and equilibrium, respectively. V (L) is the volume of the solution and W (mg) is the amount of dry adsorbent.

RESULTS AND DISCUSSION

Characterization of HA and Ag doped HA

The FTIR spectra of HA and Ag doped HA were recorded at 4000-500 cm^{-1}. The functional groups present in the HA and Ag dopedHA were shown in Fig. 2. From FTIR of HA (Fig 2 a) the absorption strong peak around 1035 cm^{-1} is assigned PO_4^{3-} and bands of 547 cm^{-1} and 604 $cm^{-1}$are assigned to symmetric P-O stretching[36].The broad band around 3440 cm^{-1} is the stretching mode of hydrogenbonded OH seen in both the spectra 2a and 2b. In the Ag doped HA (Fig. 2b) bands of HA (1035 cm^{-1}, 670 cm^{-1} and 547 cm^{-1}) also were observed. The peak 1647 cm^{-1} and broad bands for adsorbed water (3000– 3500 cm^{-1}) are the evidence of water absorption due to the high specific surface area of Ag doped HA. The Ag doped HA powders exhibited FTIR patterns similar to that of und oped HA, as shown in Fig. 2b [37-39].

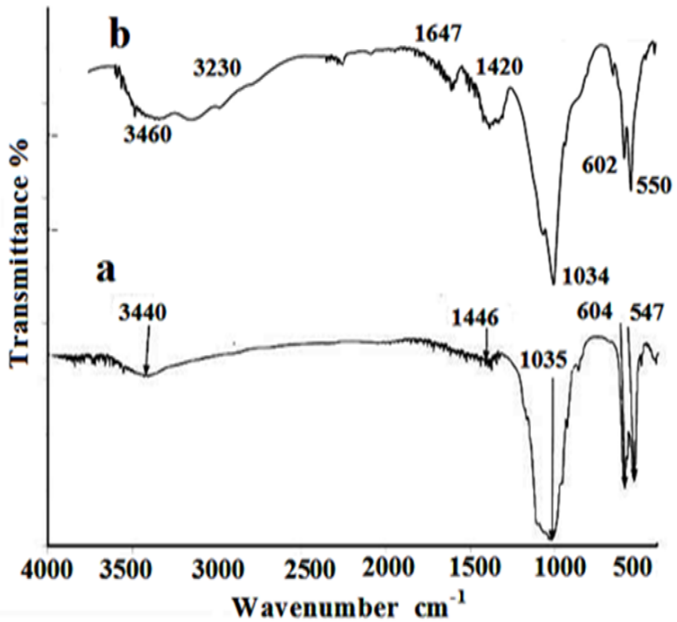

Fig. 2: FTIR of a-HA and b-Ag doped HA

The scanning electron micrograph of HA and Ag doped HA are given in Fig. 3. The micrograph reflected the butterfly shape of the particles which were aggregated with many nanoparticles, producing a surface with porous structure. It has holes with small openings on the surface(Fig. 3a).While after Ag incorporating of HA, the micrograph showed different shapes for the particles with greater size and high aggregates and more porous structure due to the presence of the Ag ions (Fig. 3b).EXD of HA and Ag doped HA (Fig. 4) also confirmed the existence of Ag on the surface of HA.

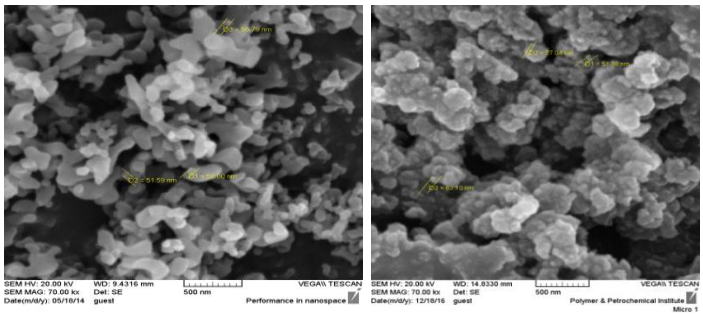

a b

Fig. 3: SEM of a-HA and b-Ag doped HA

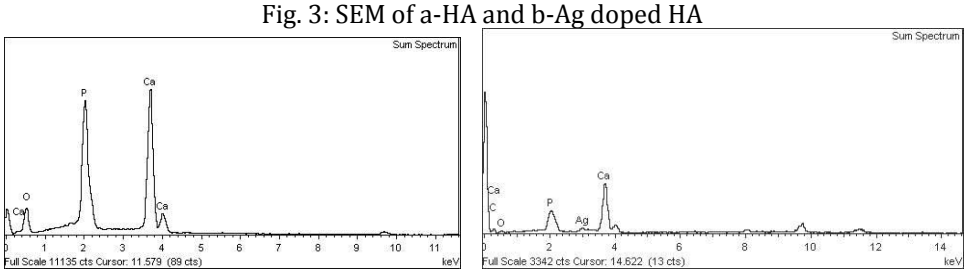

a b

Fig. 4: EXD of a- HA and b-Ag doped HA

X-ray powder diffraction analysis was conducted to analyze phase purity and phase composition of the HA and Ag doped HA structures. XRD patterns of the HA and doped HA are shown in Fig. 5.The X-ray diffraction pattern were recorded and verified using standard PDF card # 9-432 for hydroxyapatite. The XRD pattern of Ag doped HA shows combined features from the XRD patterns of HA and Ag, suggesting that Ag ions were attached to HA and the crystalline structure of HA was well preserved even after incorporating of Ag on the HA. A slight reduction of peak intensity counts for Agdoped HA is in agreement with a similar behavior of the literature [33],and the small molar amount (2%mol) of Ag does not influence significantly the cell parameter values. The HA had Hexagonal unit cell structure (a=b=9.41500, c= 6.87900, α= β=90, γ= 120, Primitive - P63/m) and Ag doped HA had hexagonal unit cell structure (a=b=9.423, c=6.881 and α=β=90, γ=120, primitive, p63/m). These values were in close proximity with unit cell dimensions of HA crystals reported previously in the literature [40]. Almost identical patterns were recorded for both compositions, which suggest that the presence of Ag did not change phase-purity of HA. The HA exhibited several high intensity peaks corresponding to various planes of HAviz., i.e. (211), (002), (202), (220), and (240). Compared to XRD pattern of pure HA, the crystallinity of HA powders increased on addition of Ag but no obvious phase change was noticed in their XRD patterns. The mean crystallite size (D) of particles was calculated from the XRD line broadening measurement using the Scherrer equation:

$$D = 0.89\,\lambda/\beta \cos\theta$$

Where, λ is the wavelength (Cu-K_α), β is the full width at the half maximum of the HA (002) line and θ is the diffraction angle. The mean particle size were about 35-65 nm.

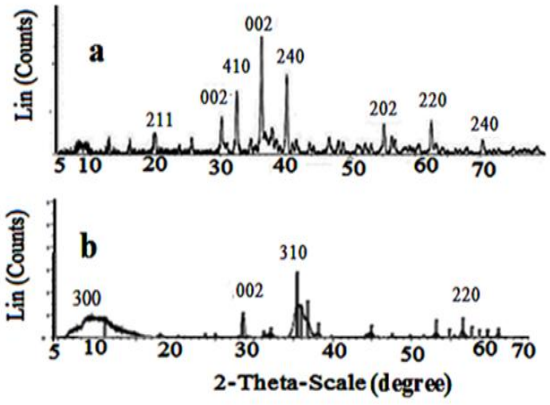

Fig. 5: XRD pattern of A-HA and B-Ag doped HA

The N_2 adsorption–desorption isotherms and pore size distributions of Ag doped HA is shown in Fig. 6. The sample exhibited typical IV type isotherms and H1 type hysteresis loops at high relative pressures. This indicates that Ag doped HA with large pore size distribution was successfully prepared. Table 1 shows the characterization of HA and Ag doped HA.

Table 1: Characterization of HA and Ag doped HA

Characterization		samples	
		HA	Ag doped HA
	Surface area (m^2/g)	81.5	100.88
	Correlation coefficient (R^2)	0.994	0.990
BJH adsorption summary	Surface area (m^2/g)	96.652	96.334
	Pore volume (cm^3/g)	0.346	0.336
	Pore diameter (nm)	8.45	8.04
BJH desorption summary	Surface area (m^2/g)	117.6	107.88
	Pore volume (cm^3/g)	0.355	0.348
	Pore diameter (nm)	9.53	9.21

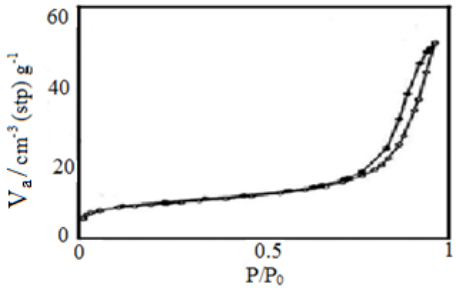

Fig. 6: N_2 adsorption–desorption isotherms ofAg doped HA

Adsorption Study

Effect of Contact Time

Effect of contact time on the adsorption of MR onto HA and Ag doped HA was investigated. The results of sorption studies, carried out as a function of contact time are presented in Fig. 7.a.The adsorption of MR is rapid from the beginning of the experiment and thereafter it proceeds at a slower rate and finally reaches to equilibrium. The results showed the rate of adsorption is initially rapid with most of the dye being adsorbed within~40 % for HA at 60 min of contact time and 78 % for Ag doped HA at contact time 40 min, respectively. For following experiences contact time of 40 min was designated. Fig. 7.also is shown Ag doped HA had higher adsorption capacity than HA. It looks removal of dye was occurred on the outer surface of the adsorbent [41]. This is due the higher surface area of Ag doped HA than HA. Fig. 7.b. also shows the MR adsorbed onto Ag doped HA.

The results of BET characterization are shown at Table. 1.The specific surface area (BET method) of HA and Ag doped HA were 81.5 and 100.88 $m^2\ g^{-1}$, respectively. Doped of Ag into the HA increased the surface area of sorbent, therefore the contact time of MR with Ag doped HA was decreased.

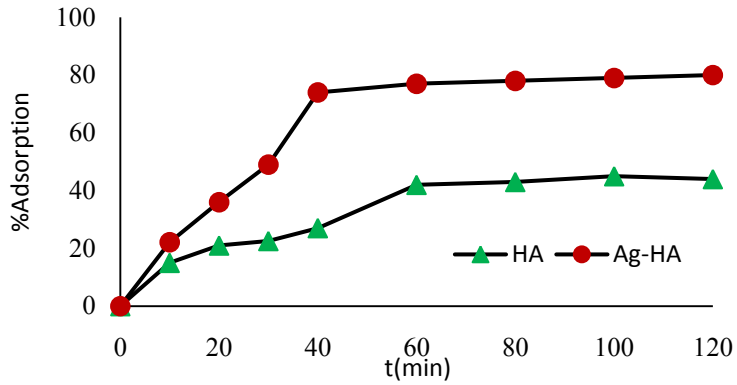

Fig. 7: a. Effect of contact time on the adsorption of MR onto HA and Ag doped HA (30 mL of MR 50 mg L^{-1}, 0.1 g sorbent)

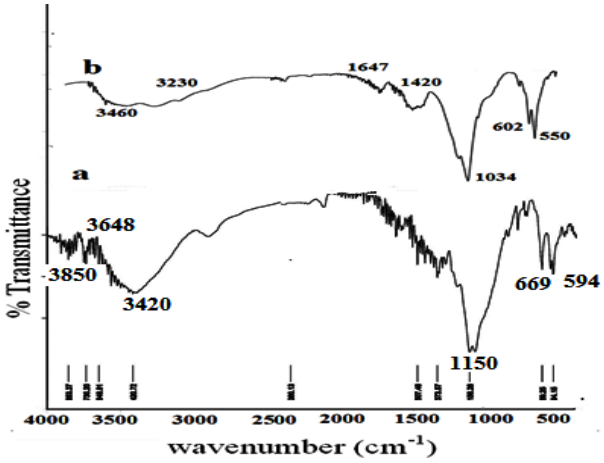

Fig. 7: b. FTIR of a-Ag doped HA and b-Ag doped HA adsorbed MR

Effect of Initial Dye Concentration

The effect of MR dye concentration (5-100 mg L^{-1}) was studied by adding 0.1g of adsorbate at mixing rate 150 rpm. The equilibrium adsorption capacity of the adsorbent for MR increases with increasing initial dye concentration from 5-50 mg L^{-1}.This is probably due to a high driving force for mass transfer in high dye concentration. The results also showed adsorption concentrations of more than 50 mg L^{-1}did not causes the higher adsorption capacity for MR.

Effect of pH on Dye Adsorption

The pH of the dye solution is an important parameter controlling the adsorption capacity of dye. Effect of pH on adsorption of MR by using initial dye concentration50mg $L^{-1}$and shaking time of 40 min was studied. Effect of pH (2 -10) for adsorption of MR on HA and Ag doped HA at 25°C is given in Fig. 8.It can be observed that the adsorption capacity of two adsorbents increase with an increase in pH of the initial solution from 2 to 7, and then reach gradually constant as the pH become basic. The pHs ≥ 7 is favorable for adsorption process of MR. High adsorption of dye indicates that, the surface of nanoparticles seems to be basic. MR is azo anionic dye, which exist in aqueous solution in the form of negatively charged ions.

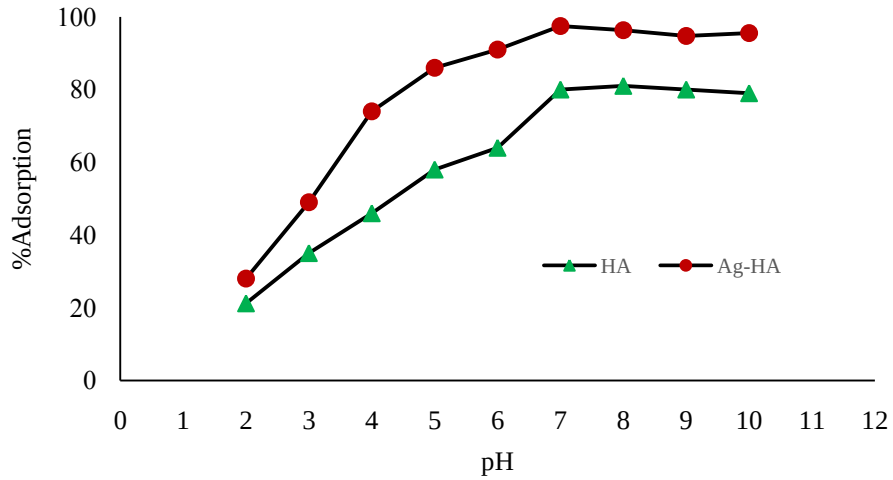

Fig. 8: Effect of pH on the adsorption of MR onto HA and Ag doped HA
(30 mL of MR 50 mg L^{-1}, pH 7, 0.1 g sorbent)

Effect of Adsorbent Mass

To determine the effect of sorbent dosage on adsorption, dye concentration of 50mg L^{-1} and samples with different sorbent dosages ranging from 0.01 to 0.2 g under constant temperature at 25°C, contact time 40 min and pH 7were studied. The effect of adsorbent mass is shown in Fig. 9. The results indicate that percentage of dye adsorption increased with increase of adsorbent dose from 0.01-0.1 g, while q_e decreased. The increasing availability of the binding sites with increased adsorbent dose may be responsible for increase in percent removal of the dye. However, the gradual decrease in q_e may be as a result of decreased ratio of MR molecules per active adsorption site, and/or due to decrease in total surface area because of agglomeration of adsorbent. Similar increase in percent removal and decrease in q_e with increase in adsorbent dose has been reported [42].

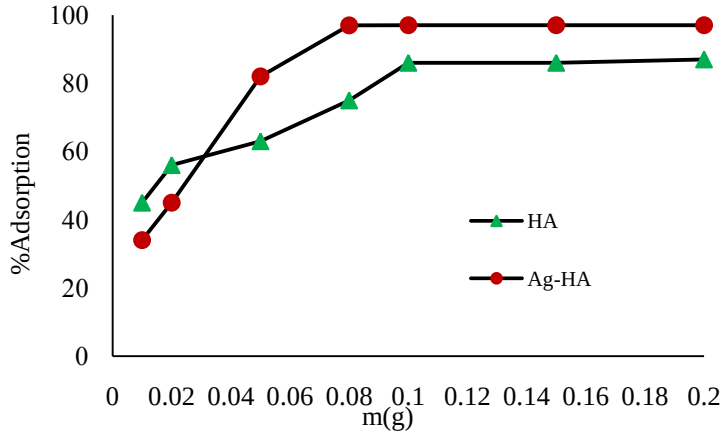

Fig. 9: Effect of mass of sorbent (Contact time 40 min, pH 7, MR 50 mg L^{-1} and temperature 25 ˚C)

Effect of Temperature

Removal of MR by HA and Ag doped HA was performed by varying temperatures (20-70˚C). Adsorption of MR on HA and Ag doped HA was enhanced by increasing the temperature from 20 ˚C to 40 ˚C. Fig. 10 shows that adsorption capacity decreased with increasing temperature from 50-80 ˚C. This may be due to desorption of MR dye from surface of sorbents. Thermodynamic parameters were determined by investigation effect of temperature on carmine adsorption.

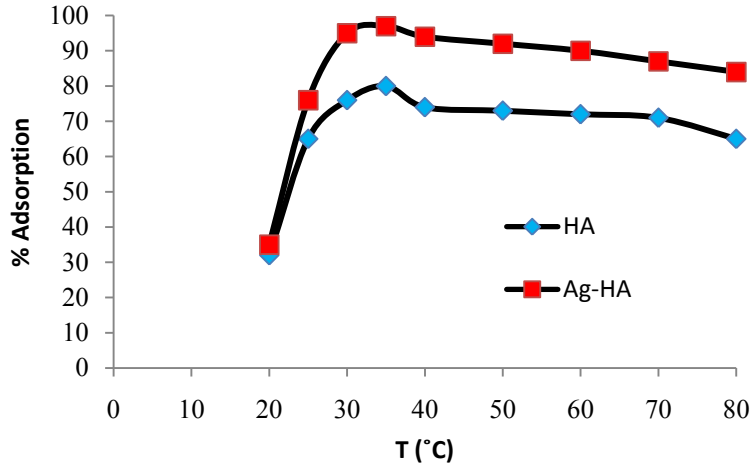

Fig. 10: Effect of temperature (Contact time 40 min, pH 7, MR 50 mg L^{-1} and 0.1 g sorbents)

Thermodynamic Study

Thermodynamic parameters, i.e. free energy change(ΔG^{o}), standard enthalpy change (ΔH^{o}) and entropy change (ΔS^{o}), vary with the thermodynamic equilibrium constant (K_c). The determination of Gibb's free energy is very important to determine the feasibility of the adsorption process along with standard enthalpy change (ΔH^{o}), standard entropy change (ΔS^{o}).The Gibbs free energy change ΔG^{o} of adsorption process can be calculated from classic Van't Hoff equation [43]:

$$\Delta G^{o} = -RT \ln K_c \quad (3)$$

$$\Delta G^{o} = \Delta H^{o} - T\Delta S^{o} \quad (4)$$

The Enthalpy change (ΔH^{o}) (i.e. heat of adsorption) and Entropy change (ΔS^{o}) is related with the Gibbs free energy by the equation:

$$\ln K_c = -\Delta G^{o}/RT = \Delta S^{o}/R - \Delta H^{o}/RT \quad (5)$$

K_c is equilibrium constant of Van't Hoff equation, can be obtained from qe / Ce. ΔG^{o} is Gibbs free energy change (KJ mol^{-1}), ΔH^{o} is Enthalpy change (KJ mol^{-1}) and ΔS° is entropy change (KJ mol^{-1} K^{-1}).A plot ln K_c Versus 1/T is given straight line, ΔH^{o} and ΔS° can be determined from slope and intercept, respectively (Fig. 11). Table 2 shows thermodynamic parameters of adsorption of MR by HA and Ag doped HA. The negative value of ΔG^{o} indicates the feasibility and spontaneous nature of the adsorption process and more negative values indicate that adsorption process becomes more spontaneous with rise in temperature, which favors for adsorption process. The positive value of ΔS^{o} describes the randomness during adsorption process and reflects the affinity of adsorption of MR dye and confirms the increasing

randomness at the solid–solution interface during adsorption. The positive value of ΔH° confirms the endothermic nature of the adsorption process [44, 45].

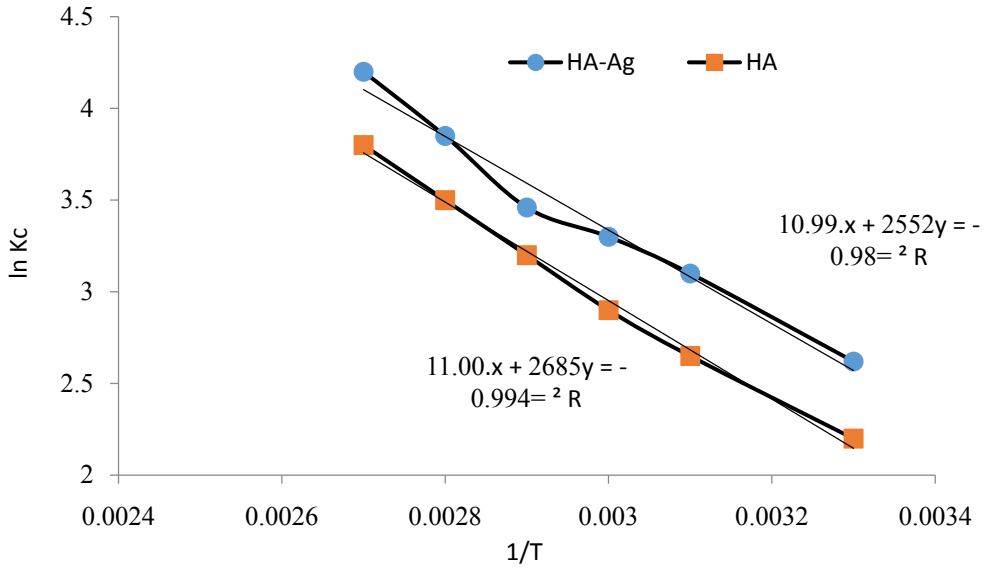

Fig. 11: Plot of $\ln K_c$ verses 1/T

Table 2: Thermodynamic parameters for adsorption of MR by HA and Ag doped HA

ΔS° (J mol^{-1}K^{-1})	ΔH° (J mol^{-1})	ΔG° (KJ mol^{-1})	T (K)	Sorrbent
1.33	323	-80	303	HA
		-93.3	313	
		-106.6	323	
		-120	333	
		-133.2	343	
		-146.5	353	
1.323	307	-93.9	303	Ag doped HA
		-107	313	
		-120.33	323	
		-133.56	333	
		-146.8	343	
		-162.5	353	

Kinetic of Adsorption

Adsorption kinetics provides the information about adsorption pathway. In the present study, In order to predict the adsorption behaviors, pseudo first order (Sharma, 2011) and pseudo second order (Ho et al, 2000, Ho, 2006)kinetic models were used to fit the experimental data. The models were given the following equations:

$$\ln (q_e - q_t) = \ln q_e - k_1 t \quad (6)$$

$$t/ q_t = t/q_e + 1/(k_2 q_e^2) \quad (7)$$

Where, q_e is adsorbate amount absorbed on per unit mass of adsorbent at equilibrium and and q_t(mg g^{-1}) is the adsorbate amount absorbed on per unit mass of adsorbent at time t (min),k_1 (min^{-1}) and k_2 (g mg^{-1} min^{-1}) are the pseudo first order and pseudo second order rate constants, respectively. Furthermore, for the pseudo second order kinetic model, the half adsorption time ($t_{1/2}$) and the initial adsorption rate

(*H*) are given by the following relationships (Eqs.(8) and (9))(Ahmad Khan et al. 2018). The value of $t_{1/2}$ is the time required to uptake half of the maximal adsorbed amount of adsorbateat equilibrium and characterizes the adsorption rate well.

$$T_{1/2} = 1/ k_2 q_e \quad (8)$$

$$H = k_2 q_e^2 \quad (9)$$

The experimental data of adsorption of MR on HA and Ag doped HA were studied with above two kinetic models and the results were shown in Figs. 12a and 12 b. The acceptability and hence the best fit model for the kinetic data were based on the square of the correlation coefficients $R^2$and the percentage error function. Table 3 also shows the R^2 and rate constant of adsorption. The results showed the pseudo second order kinetic model was suitable to describe the adsorption behaviors of MR on sorbents(Ahmad Khan et al. 2018).

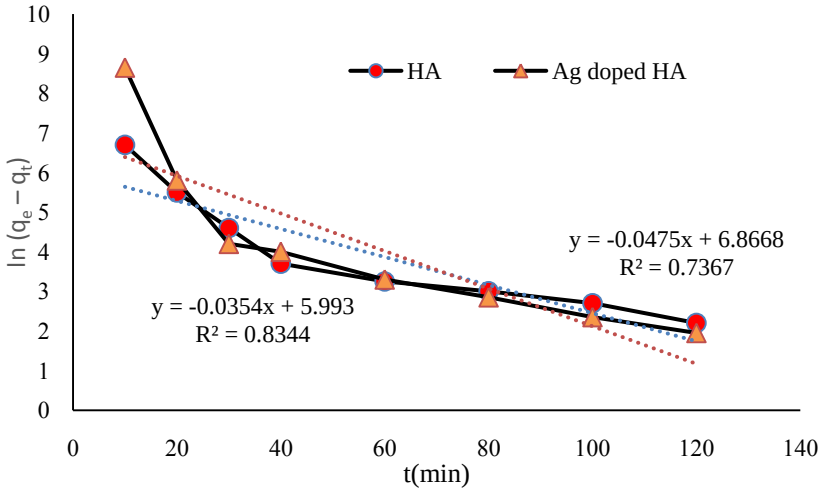

Fig. 12: a.) Pseudo first order kinetics for adsorption of MR onto HA and Ag doped HA (30 mL of MR 50 mg L^{-1}, pH 7, 0.1 g sorbent)

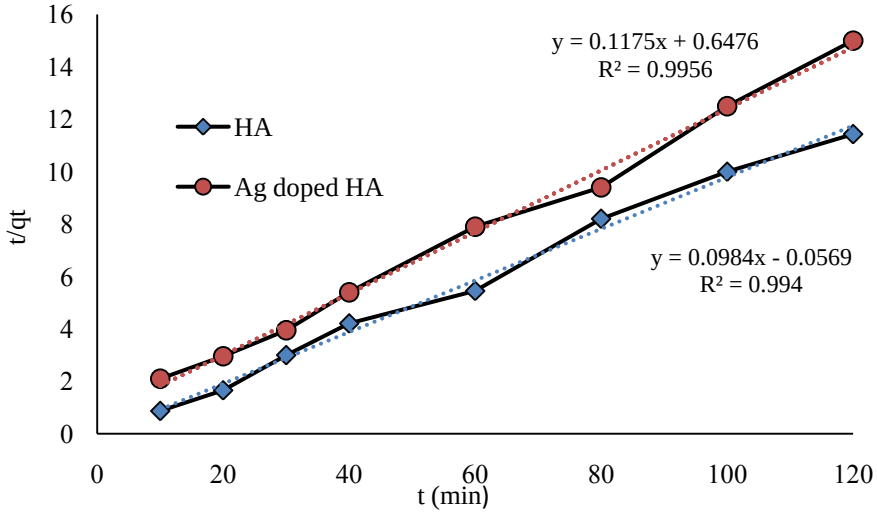

Fig. 12b). Pseudo second order kinetics for adsorption of MRonto HA and Ag doped HA(30 mL of MR 50 mg L^{-1}, pH 7, 0.1 g sorbent)

Table 3: Kinetic parameters for adsorption of MR by HA and Ag doped HA

Sorbent	First order		Second order			
	R^2	K_1 (min^{-1})	R^2	K_2 (g mg^{-1} min^{-1})	$T_{1/2}$	H
HA	0.834	3.4×10^{-2}	0.994	1.7×10^{-1}	0.579	17.55
Ag doped HA	0.736	4.7×10^{-2}	0.995	2.1×10^{-2}	5.6	1.5

Adsorption Isotherm

Equilibrium relationship between the amounts of dye adsorbed on the surface of an adsorbent could be recognized through adsorption isotherms. In the present study, the Freundlich and Langmuir isotherm models were applied to the adsorption data. The Freundlich model is applicable to heterogeneous system

and it involves the formation of multi layers. The Freundlich adsorption isotherm is given by equations of 10 and 11:

$$q_e=K_F\,Ce^{1/n} \quad (10)$$

$$\ln q_e=\ln K_F + 1/n \ln C_e \quad (11)$$

Where, q_e is the solid phase equilibrium concentration (mg g^{-1}); C_e is the liquid equilibrium concentration of dye in solution (mg L^{-1}); K_F is the Freundlich constant representing the adsorption capacity (mg g^{-1}), and n is the heterogeneity factor showing adsorption intensity. The values of K_F and n can be obtained from slope and intercept of linear plot of ln q_e versus ln C_e and values are given in Table 4.

The assumption of Langmuir model is that the formation of monolayer take place on the surface of the adsorbent, indicating that only one dye molecule could be adsorbed on one adsorption site. The Langmuir adsorption model is given as:

$$C_e/q_e=1/ (K_Lq_m)+(C_e/K_L) \quad (12)$$

Where, q_e and C_e are defined as above, K_L is the equilibrium adsorption constant related to the affinity of binding sites (L mg^{-1}); and q_m is the maximum amount of dye per unit weight of adsorbent for complete monolayer coverage (mg g^{-1}).The values of q_m and K_L can be obtained from slope and intercept of the linear plot of C_e/q_e versus C_e (Table 4).

Table 4 shows the calculated values of Langmuir and Freundlich model's parameters. The adsorption isotherm of sorbents could be described well by both Langmuir and Freundlich equations, but the comparison of correlation coefficients (R^2) of both equations indicates Freundlich model had better fit for the experimental equilibrium adsorption data than the Langmuir model.

Table 4: Langmuir and Freundlich constants for the adsorption of MR by HAAg doped HA

Sorbent	Freundlich			Langmuir		
	K_F	n	R^2	q_m (mg g^{-1})	K_L (L mg^{-1})	R^2
HA	1.96	0.99	0.98	588	1.82×10^{-5}	0.934
Ag doped HA	2.52	1	0.999	524	1.35×10^{-5}	0.942

Removal of MR from Real Wastewater

Adsorption efficiency of the Ag doped HA was checked with real wastewater containing MR dye. Real wastewater (five different samples) was collected in polypropylene bottle from local textile dyeing unit (Yazdbaf, ano, aftab, Ardakan and Azartabof IRAN) and stored at 4 °C in a refrigerator. The samples were filtered using 0.45 μm membrane. MR (50 mg) was added into one liter of real wastewater, to confirm MR concentration in wastewater. The adsorption experiments with different wastewater samples were performed at the optimized conditions. The percent removal of MR from different real textile wastewater sample was about 15~20 % lower than that of the synthetic wastewater under similar conditions. This decrease in percent removal may be due to the presence of several other types of dyes and salts such as chloride, sulphate, calcium and magnesium ions as impuritiesin the sample that may compete with MR molecules for adsorption.

Desorption and reusability of Adsorbent

Reusability of sorbent is one of the highest importances in adsorption studies. The Ag doped HAwas regenerated by calcination at 300 ˚C for 2h. For this purpose, 30 mL of MR 50 mg L^{-1}loaded adsorbent was equilibrated for 60 min. After 20 min, 65% of dye was desorbed while 98% of dye was desorbed after 45 min. The desorbed concentration of MR was estimated spectrophotometrically. The adsorption efficiency of the regenerated adsorbent decreased with increasing desorption cycle. Almost 64% of dye was adsorbed at fifth cycle for Ag doped HA.

CONCLUSION

HA and Ag doped HA were sucsesfully prepared by chemical wet method. They were used as sorbent for removal of MR as an azo dye from aqueous solutions. Ag doped HA was a useful adsorbent for removing MR from aqueous solution. The adsorption capacity of MR was higher by Ag doped HA than HA. The maximum removal efficiency was 82% and95% at50 gL^{-1} for HA and Ag doped HA, respectively. pH played an important role in the removal of MR. The removal efficiency in nuteral to alkal in solution (pH ≥7) was higher than that in acidic solutions. The adsorption thermodynamic showed that the adsorption becomes more feasibility and randomness with increasing in temperature. The adsorption process on the Ag doped HA was endothermic. The adsorption kinetics of MR on both HA and Ag doped HA followed by

second order model. It was found that the adsorption isotherm of sorbents could be described well by both Langmuir and Freundlich equations. However, the Freundlich isotherm fitted better than the Langmuir isotherm model. Ag doped HA can acts as a reusable and friendly environment sorbent for dye removal.

ACKNOWLEDGMENTS

The authors wish to thank Islamic Azad University of Yazd (IAUY) for the financial support of this work. Also, thank co-workers and technical staff of the chemical department for help during various stages of this work.

REFERENCES

[1] KornarosM, Lyberatos G, Biological treatment of wastewaters from a dye manufacturing company using a trickling filter, *J. Hazard. Mater.* 136(1), 95–102 (2006).

[2] Gadekar M. R., Ahammed M. M., Coagulation/flocculation process for dye removal using water treatment residuals: modelling through artificial neural networks, *Desal Water Treat.* 55 (57), 26392-26400 (2016).

[3] Pan F, Liu, Wang W, Yang L, Treatment of Orange G dye wastewater by electrochemical process with auxiliary coagulation, *Chin J Environ Eng,* 7(10), 3713-3718 (2013).

[4] Nourmoradi H, Zabihollahi S, Pourzamani H.R, Removal of a common textile dye, navy blue (NB), from aqueous solutions by combined process of coagulation–flocculation followed by adsorption, *Desal. water treat.* 57(11), 1-12 (2015).

[5] Cheng L, Wei M, Huang L, Pan F, Xia D, Li X, Xu A,Efficient H2O2oxidation of organic dyes catalyzed by simple copper(ii) ions in bicarbonate aqueous solution, *Ind. Eng. Chem. Res.* 53 (9), 3478–3485 (2014).

[6] Inchaurrondoa N, Fontb J, Ramosc C.P, Haure P, Natural diatomites: Efficient green catalyst for Fenton-like oxidation of Orange II, *Applied Catalysis B: Environment,* 181, 481–494 (2016).

[7] Esteves B. M, Rodrigues C. S.D, Boaventura R. A. R, maldonado-hodar F.J, Madeira L. M, Coupling of acrylic dyeing wastewater treatment by heterogeneous Fenton oxidation in a continuous stirred tank reactor with biological degradation in a sequential batch reactor, *J. Environ. Manag.,* 166, 193-203 (2016).

[8] Meric S, Lofrano G, Belgiorno V, Treatment of reactive dyes and textile finishing wastewater using Fenton's oxidation for reuse, *Inter. J. Environ. Pollut,* 23 (3), 248-253 (2005).

[9] Hashemian S, Dehghanpor A, Moghahed M, Cu0.5Mn0.5Fe2O4nanospinels as potential sorbent for adsorption of brilliant green, *J. Indust. Eng. Chem.* 24, 308–314 (2015).

[10] Vučurović V, Razmovski' R, Miljić U, Puškaš V,Removal of cationic and anionic azo dyes from aqueous solutions by adsorption on maize stem tissue, *J Taiw Inst Chem Eng,* 45(40), 1700-1708 (2014).

[11] Abo El Naga A. O. , ShabanS. A,El KadyFathy Y.A, Metal organic framework-derived nitrogen-doped nanoporous carbon as an efficient adsorbent for methyl orange removal from aqueous solution, *J Taiw. Inst. Chem. Eng.*, 93, 363-373 (2018).

[12] Hashemian S, Rahimi M, Kerdegari A. A,CuFe2O4@graphene nanocomposite as a sorbent for removal of alizarine yellow azo dye from aqueous solutions, *Desal.Water Treat.*, 57, 14696–14707 (2016).

[13] Hashemian S, Foroghimoqhadam A, Effect of copper doping on CoTiO3Ilmenite type nano particles for removal of Congo red from aqueous solution, *Chem. Eng. J.* 235, 299–306 (2014).

[14] Liew Abdullah A.G, MohdSalleh M. M, Sitimazlina M. K, MegatMohd Noor M. J, Osman M. A. R, Wagiran R, Sobri S, Azo dye removal by adsorption using waste biomass: sugarcane bagasse, *Inter. J. Eng. Technol.* 2(1), 8-13 (2005).

[15] Terangpi P, Chakraborty S, Adsorption kinetics and equilibrium studies for removal of acid azo dyes by aniline formaldehyde condensate, *Appl. Water Sci.* 7(7),3661–3671 (2017).

[16] Saxena R, Sharma S, Adsorption and kinetic studies on the removal of methyl red from aqueous solutions using low-cost adsorbent: Guargum Powder, *Inter. J. Sci. Eng. Res.* 7(3), 675-683 (2016).

[17] Nguyen V. C, Pho Q. H, Preparation of magnetic hydroxyapatite nanoparticles coated chitosan and application for adsorption of reactive blue 19 and Ni2+ ions. *The Sci. World J.* Article ID 273082, 9 pages (2014).

[18] Ramesh S. T, Rameshbabu N, Gandhimathi R, Nidheesh P. V, Srikanth K. M, Kinetics and equilibrium studies for the removal of heavy metals in both single and binary systems using hydroxyapatite, *Appl. Water Sci.* 2,187–197(2012).

[19] Hasegawa M, Sudo A, Komlev V. S, Barinov S. M, Uchida A, High release of antibiotic from a novel hydroxyapatite with bimodal pore size distribution. *J. Biomed. Mater.Res.* B, 70, 332–339 (2004).

[20] Chai F, Hornez J.C, Blanchemain N, Neut C, Descamps M, Hildebrand H. F, Antibacterial activation of hydroxyapatite (HA) with controlled porosity by different antibiotics, *Biomol. Eng.* 24 (5), 510–514 (2007).

[21] Kumar N.A, Kumar S, Hydroxyapatite-ciprofloxacin minipellets for bone-implant delivery: preparation, characterization, in-vitro drug adsorption and dissolution studies, Inter. *J. Drug Devel. Res.* 1(1), 47-59 (2009).

[22] Yin A, Margolis H.C, Grogana J, Yao Y, Troxler R. F, Oppenheim F. G, Physical parameters of hydroxyapatite adsorption and effect on candidacidal activity of histcatins, *Arch. Oral Biol.* 48, 361–368 (2003).

[23] Bekkali C. E., BouyarmaneH., ElKarbane M., Masse S., Saoiabi A, Coradin T. Laghzizil A., Zinc oxide-hydroxyapatite nanocompositephotocatalysts for the degradation of ciprofloxacin and ofloxacin antibiotics, *Coll. Surf. A: Phys. Eng. Aspe.* 539, 364- 370 (2018).

[24] Dybowska A, Manning D.A.C, Collins M.J, Wess T, Woodgate S, Valsami-jones E, An evaluation of the reactivity of synthetic and natural apatites in the presence of aqueous metals, *Sci. Total Environ.,* 407, 2953–2965 (2009).

[25] Feng Y, GongaJ. L, Zeng G.M,NiuQ.Y, Zhang H.Y, Niu C. G, Deng J.H, Yan M, Adsorption of Cd (II) and Zn (II) from aqueous solutions using magnetic hydroxyapatite nanoparticles as adsorbents, *Chem Eng J,* 162, 487–494 (2010).

[26] Corami A, Mignardi S, Ferrini V, Copper and zinc decontamination from single and binary-metal solutions using hydroxyapatite, *J Hazard Mater,* 146, 164–170 (2007).

[27] Aliabadi M, Irani M, Ismaeilic J, Najafzadeh S, Design and evaluation of chitosan/hydroxyapatite composite nanofiber membrane for the removal of heavy metal ions from aqueous solution, *J Taiw Inst Chem Eng,* 45 (2), 518-526 (2014).

[28] Gomez del Rio J. A, Morando P.J, Cicerone D.S, Natural materials for treatment of industrial effluents: comparative study of the retention of Cd, Zn and Co by calcite and hydroxyapatite. Part I: batch experiments, *J Environ Manag,* 71, 169–177 (2004).

[29] Allam K, El Bouari A, Belhorma B, BihL, Removal of methylene blue from water using hydroxyapatite submitted to microwave irradiation, *J. Water Res Prot,* 8, 358-371 (2016).

[30] Chen Y, Lan T, Duan L, Wang F, Zhao B, Zhang S, Wei W, Adsorptive removal and adsorption kinetics of fluoroquinolone by nano-hydroxyapatite, *PLoS One,* 10(12), e0145025 (2015).

[31] Suzuki T, Hatsushika T, Lattice ion reaction characteristics of hydroxyapatite for iron (+2), iron (+3) and lead (+2) ions in acidic aqueous solutions, *Gypsum Lime,* 224, 15-20 (1990).

[32] Zhao L, Chu P. K, Zhang Y, Wu Z, Antibacterial coatings on titanium implants, *J BiomedMaterRes Part B: Appl. Biomat.* 91, 470-480 (2009).

[33] Ciobanu1 C. S, Massuyeau F, Constantin L. V, Predoi D, Structural and physical properties of antibacterial Ag-doped nano-hydroxyapatite synthesized at 100°C, Nano scale Res Lett, 6, 613-620 (2011).

[34] Rey C, Lian J, Grynpas M, Shapiro F, Zulkerg L, Glimcher M. J, Non-apatitic environments in bone mineral: FT-IR detection, biological properties and changes in several disease states, *Conn Tissue Res,* 21, 267–273(1989).

[35] Barka N, Qourzal S, Assabbane A, Nounah A, Ait-Ichou Y, Removal of reactive yellow 84 from aqueous solutions by adsorption onto hydroxyapatite, *J Saudi Chem Soc,* 15(3), 263–267(2011).

[36] Fowler B.O,Infrared studies of apatites. I. Vibrational assignments for calcium, strontium, and barium hydroxyapatites utilizing isotopic substitution, *Inorg Chem* 13, 194–207(1974).

[37] Mitsionis A, Vaimakis T, Trapalis C, Todorova N, Bahnemann D, Dillert R, Hydroxyapatite/titanium dioxide nanocomposites for controlled photocatalytic NO oxidation, *Appl Cat B: Environ,*106, 398– 404(2011).

[38] Arumugam S. K, Sastry T. P, Sreedhar B, Mandal A. B, One step synthesis of silver nanorods by autoreduction of aqueous silver ions with hydroxyapatite: an inorganic–inorganic hybrid nanocomposite, *J Biomed Mat Res Part A,* 391-398(2007).

[39] HuangY, Zhang X, Mao H, Li T, Zhao R, Yan Y, Pang X, Osteoblastic cell responses and antibacterial efficacy of Cu/Zn co-substituted hydroxyapatite coatings on pure titanium using electrodeposition method, *RSC Advance,* 5, 17076–17086 (2015).

[40] Padmanabhan S. K, Balakrishnan A, Chu M. C, Lee Y. J, Kim T. N, Cho S. J, Sol–gel synthesis and characterization of hydroxyapatite nanorods, *Particu.* 7, 466–470 (2009).

[41] Sivaraj R, Namasivayam C, Kadirvelu K, Orange peel as an adsorbent in the removal of Acid violet 17 (acid dye) from aqueous solutions, *Waste Manag,* 21(1), 105-110 (2001).

[42] Ahmed F, Dewani R, Pervez M. K, Mahboob S. J, Soomro S. A, Non-destructive FT-IR analysis of mono azo dyes, *Bulg Chem Comm,* 48 (1), 71 –77 (2016).

[43] Ahmad Khan E, Shahjahan, Alam Khan T, Adsorption of methyl red on activated carbon derived from custard apple (Annonasquamosa) fruit shell: Equilibrium isotherm and kinetic studies, *J Molec Liquids,* 249, 1195–1211 (2018).

[44] Joshi P, Manocha S, Kinetic and thermodynamic studies of the adsorption of copper ions on hydroxyapatite nanoparticles, *Mater Today: Proce.,* 4(9), 10455-10459 (2017).

[45] Sharma Y. C,Adsorption characteristics of a low-cost activated carbon for the reclamation of colored effluents containing malachite green, *J Chem Eng Data,* 56 (3), 478–484 (2011).

[46] SharmaP, Kaur H, SharmaM, SahoreV, A review on applicability of naturally available adsorbents for the removal of hazardous dyes from aqueous waste, *Environ Monit Assess,* 183(1-4), 151-195 (2011).

[47] Ho Y.S, Ngj. C. Y, Mckay G, Kinetics of pollutant sorption by biosorbents: review, *Sep Purif Method,* 29 (2), 189–232 (2000).

[48] Ho Y. S, Review of second-order models for adsorption systems, *J. Hazard Mater,* 136, 681-689 (2006).